Landform Analysis 44: 43–56
doi: 10.12657/landfana-044-002
Received: 2025.11.04; Accepted: 2025.12.05

LiDAR-based DEM visual interpretation as a tool for landslide mapping – example of problems with landslide identification and its verification with electrical resistivity tomography

Paweł Kroh [1], Marta Kondracka [2], Dariusz Ignatiuk [2]

[1] Institute of Biology and Earth Sciences, University of the National Education Commission, Krakow, Poland; pawel.kroh@uken.krakow.pl
[2] Institute of Earth Sciences, Faculty of Natural Sciences, University of Silesia in Katowice, Sosnowiec, Poland

Abstract: LiDAR-based Digital Elevation Models (DEM) have become one of the most valuable sources for landslide mapping. However, the delineation of landforms is not always clear. The study aims to apply DEM for landslide mapping, verified through field investigations and geophysical surveys. Visual interpretation of DEM, manual vectorization, and electrical resistivity tomography (ERT) profiles was performed in this research. While visual interpretation proves to be a highly effective method, it is not without limitations. ERT has demonstrated strong potential as a point-specific validation tool, but has limitations on shallow landslides. The study also highlights that even the highest resolution of DEM data cannot fully capture the complexity of landslide landforms.

Keywords: landslides, landslide mapping, LiDAR-based DEM, DEM interpretation, electrical resistivity tomography, Gorce Mountains, Carpathian Mountains

Introduction

Precise digital models have become a widely used data source in geomorphology (Jaboyedoff et al. 2012) and are also often used for landslide research. High-resolution light detection and ranging (LiDAR)-based digital elevation models (DEMs) seem to be the ideal tool for interpreting relief. They are very legible and so the visual interpretation of DEMs has become quite a widely used research method in landslide mapping (Eeckhaut et al. 2007, Kroh et al. 2014, Domlija et al. 2014, Leopold et al. 2017, Dolžan, Jemec Auflič 2017). DEM analysis seems to be an alternative to costly and time-consuming fieldwork (Gorum et al. 2011). Complex analysis of a Geographic Information System (GIS) and the application of automated algorithms are very interesting but they will remain the domain of researchers in the coming years. On the other hand, the visual interpretation of digital terrain models is increasingly becoming the simplest tool that is most widely used by spatial planners and other practitioners to determine the extent of landslides.

Visual interpretation of DEM continues to be the main interpretation tool at smaller scales, for practitioners, spatial planners, and researchers in geo- and biosciences who focus more on environmental studies than on modelling, the development of visual interpretation methodologies still appears to be relevant and justified. Even though research has been conducted based on such data for more than two decades, the interpretation still poses many challenges. The visual readability of the data, the possibility of 2.5D (and sometimes 3D) interpretation, and confidence in the high measurement accuracy have meant many researchers do not verify field results on a larger scale. Inconsistencies in landslide data resulting from the DEM interpretation and field mapping have also been noted by Kroh et al. (2014) and Kroh (2017, 2019) on flysch mountains, Eeckhaut et al. (2007) on wooded loess areas in Belgium, Leopold et al. (2017) on agricultural loess areas in China, and Dolžan and Jemec Auflič (2017) on the Slovenian Alpine foothills. The misinterpretations in these studies have shown, for example, that interpreters often focus only on the active parts of a landslide while ignoring its actual extent; they may interpret larger landforms (such as small valleys or catchment boundaries) as landslide areas, or fail to identify slow-moving landslides whose landforms are less distinct. Visual interpretation is a method that does not provide strict criteria for landslide delimitation. Its essence is based on the interpreter's intuition and on "reading the relief" in a DEM using geomorphological experience, without relying on clear criteria. Thanks to this approach, the method is widely used by practitioners, spatial planners, and researchers who are not experts in geoinformatics or geostatistics. The high resolution of modern DEMs and the development of their transformations (such as SVF and TPI, explained below) provide a very good balance between time efficiency and reliability. Defining strict criteria for DEM interpretation has been developed by GIS specialists and is used for automated landslide mapping, but it requires users' expertise and supervision of the algorithms. This is one of the reasons why the more "primitive" and intuitive method continues to be used and developed worldwide. While the detection of a single landslide on a homogeneous slope is not a major problem even for a layperson, the interpretation of complex landslides or various objects (both deep-seated and shallow landslides) on a larger scale is somewhat difficult. The accuracy of visual mapping can be relatively high and reaches 74% accuracy (Kroh et al. 2014), but errors in areas that are ambiguous to interpretation are difficult to avoid.

Geophysical methods have recently become a very popular tool for characterizing various geological forms. The possibility of using geophysical methods results from the fact that subsurface discontinuities like crevices, caves, and rock mass displacements cause a contrast between the surroundings, which can be observed as anomalies (geoelectric, seismic, magnetic, and gravimetric) detectable by geophysical methods (Abu-Shariah 2009). Electric, electromagnetic, and seismic methods are commonly used for studying landslide areas.

However, electrical resistivity tomography (ERT) is the most popular method used in the study of landslides. It is widely applied to: recognize the internal structure and material composition of the landslide body (Batayneh, Al-Diabat 2002, Lapenna et al. 2003, Bichler et al. 2004, Drahor et al. 2006, Jomard et al. 2007, Schrott, Sass 2008); identify the depth of the sliding surface (Suhendra et al. 2024, Sigdel, Adhikari 2020), determine the anthropogenic transformation (Sun et al. 2024, Samodra et al. 2020); recognize the degree of movement of rock masses and the impact on the infrastructure (Samodra et al. 2020, Tsai et al. 2021, Wróbel et al. 2022, Lapenna, Perrone 2022); and monitor ground saturation (Tsai et al. 2021). Sass et al. (2008) indicate that ERT is a method that provides high-resolution identification of subsurface structures, which forms the basis for a detailed and comprehensive interpretation of landslides. Pánek et al. (2010) attempted to use ERT to determine the location of active rock deformations and the internal structure. The ERT method also makes it possible to identify the mechanisms and stability of landslides and to detect the expansion joints in deformed slopes, fracture zones, less compact segments, as well as lithological-tectonic and gravity-induced structure elements (Pánek et al. 2010). Additionally, the work of Kasprzak et al. (2016, 2019) and Migoń (2017) confirmed that ERT is an effective tool for imaging subsurface structures and lithological contrasts in mountainous environments, thus highlighting its broad geomorphological applicability in the study of slope processes. On the Carpathian flysch, ERT was also used in previous research. ERT combined with DEM was successfully used by Cebulski et al. (2020) to enable a detailed reconstruction of landslide dynamics, identify movement types and active zones, and recognize a stable sandstone ridge within the otherwise mobile colluvium. Similarly, applications of ERT in landslide investigations across the Outer Carpathians by Marciniak et al. (2021) and Wróbel et al. (2022) yielded high-resolution subsurface images that facilitated the reconstruction of displacement zones and the identification of active sectors, further demonstrating the strong effectiveness of this method in Carpathian flysch settings.

Despite the increasing accuracy of LiDAR-based DEMs, misinterpretations still occur. The three study sites presented in this paper, as well as examples of other geomorphologically ambiguous terrain, aim to draw attention to the limitations of analyses based solely on geoinformatics data. This study aims to use the interdisciplinary analysis of LiDAR data for landslide mapping with verification from the visual interpretation of DEM using geophysical surveys in places with ambiguous landslide boundaries. These precise methods allow us to answer the question "Is there a landslide?" without any doubt, thus providing greater accuracy for analyses based on a DEM. This study is the first to combine DEM visual interpretation and ERT verification in Gorce National Park, filling the gap in the validation of landslide mapping methods in the region.

Both methods – visual interpretation of DEM and geophysical ERT – are popular in landslide research worldwide. Until now, DEMs have most often been used for the delimitation of landslide areas, whereas ERT, similar to other geophysical methods, has been applied to specific landslides to analyse their internal structure. The novelty of our methodological approach lies in combining these methods, which were previously used separately and at different scales, to achieve more reliable results in large-scale landslide mapping. The reliability of the results, as well as the interpretation and validation of the data used, is crucial for the development of the methodology. The authors hope that these methods will be useful for landslide researchers and practitioners, especially those working on landslide mapping using DEMs.

Study area

The massif known as the Gorce Mountains is a latitudinal mesoregion located in the central part of the Outer Western Carpathians (Solon et al. 2018). It is composed of the Carpathian flysch, from the Magura Unit (Szczęch et al. 2016), consisting of alternating sandstones, shales, and marls of the flysch series dating from the Cretaceous to the Oligocene (Forma, Zuchiewicz 2002, Oszczypko, Oszczypko-Clowes 2012) (Fig. 1). Profiles 1 and 2 are situated in an area where the bedrock is classified as the Krynica Subunit, while Profile 3 is located in an area belonging to the Bystrzycka Subunit of the Magura Unit. The research area is composed of thick-, medium-, and thin-bedded sandstones, shales, marls, and conglomerates (Forma, Zuchiewicz 2002) (Fig. 2). In general, the Gorce Mountains are intermediate mountains with strongly incised V-shaped valleys, relatively flat ridges, and steep slopes (Klimaszewski, Starkel 1972). The highest peak of the massif is Turbacz, with an elevation of 1310 m a.s.l. The foothills of the Gorce Mountains on the southern side (Orava-Nowy Targ Basin) are at an elevation of approximately 580 m a.s.l., and on the northern side, in the area of Mszana Dolna, at approximately 450 m a.s.l. Thus, the elevation differences in the massif exceed 850 meters (Kroh, Pawlik 2021). Apart from fluvial erosion, mass movements are the main factor that has reshaped the relief of the Gorce Mountains (Buczek 2019). Landslide activity in the Gorce Mountains, as in the entire Western Carpathians, is connected with humid periods during the Holocene (Margielewski 1998). The oldest dated organic matter from landslide deposits in the Gorce Mountains is approximately 11,000 cal BP (Buczek 2019) and 9,600 cal BP (Kroh et al. 2021), but landslide activity is also observed today. The largest landslide event in recent decades occurred in July 2010, when approximately 1,345 landslides were reported (Grabowski, Przybycin 2010).

Landslides in the Gorce Mountains have been studied for a long time (Kroh, Pawlik 2021) but to a lesser extent than for neighboring mountains. An important, long-term research area has been the valleys of the Jaszcze and Jamne streams, where environmental processes have been studied since the 1960s (Obrębska-Starklowa 1969, Niemirowski 1974, Gerlach 1976, Bucała et al. 2016). In the last decade, various researchers noticed the gap in the knowledge about landslides in the Gorce Mts., and several research centers are currently dealing with landslide and dating processes in these mountains. The Gorce Mountains area is covered by a detailed geological map of Poland (SMGP) at a scale of 1:50,000 (Sheets Rabka 1032, Mszana Górna 1033, Łącko 1034, Nowy Targ 1049, Krościenko 1050). The core of the massif is located on the Mszana Górna (1033) sheet, onto which landslide areas have been mapped. Most areas identified as susceptible to landslides between 1953 and 1974 (the period when field photographs were taken) were underestimated. The true extent of landslides in these mountains is much greater. Within the borders of the national park, the latest research shows the existence of 1,285 ha of landslides, but in the SMGP, there are only approximately 660 ha of landslides. This large difference may result from the methodology of work, the fact that the mapping teams focused on geological (not geomorphological) research, and that the area was heavily overgrown with vegetation, making it difficult to delimit large forms. The Gorce area located outside the national park, was mapped for landslides as part of the construction of the Landslide Counteracting System

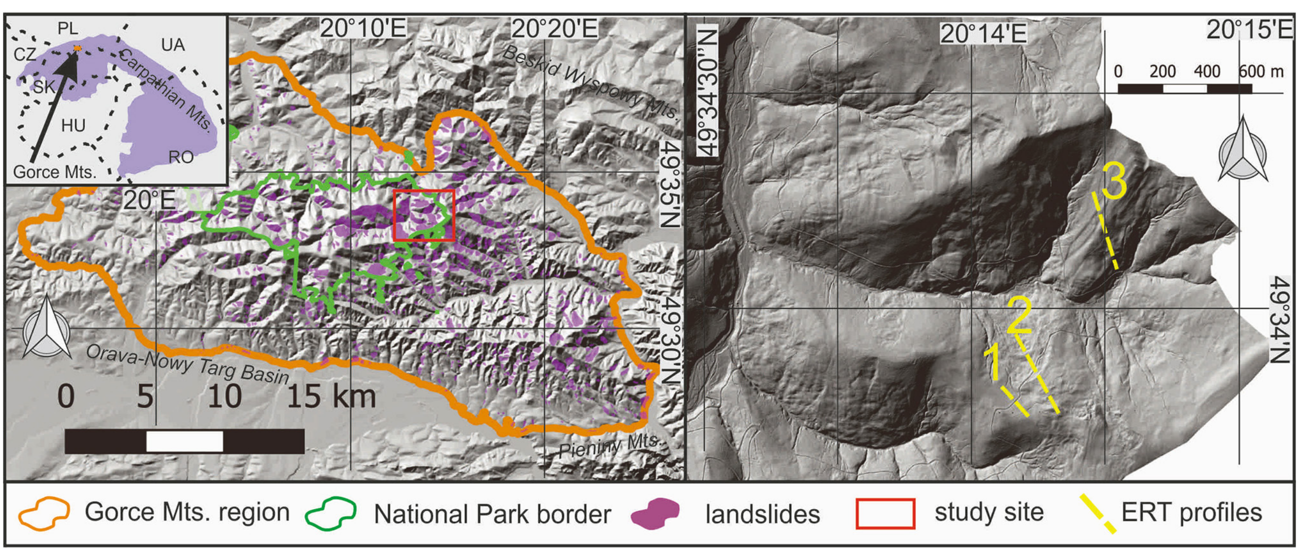

Fig. 1. Location of research area, region delineation by Solon et al. 2018

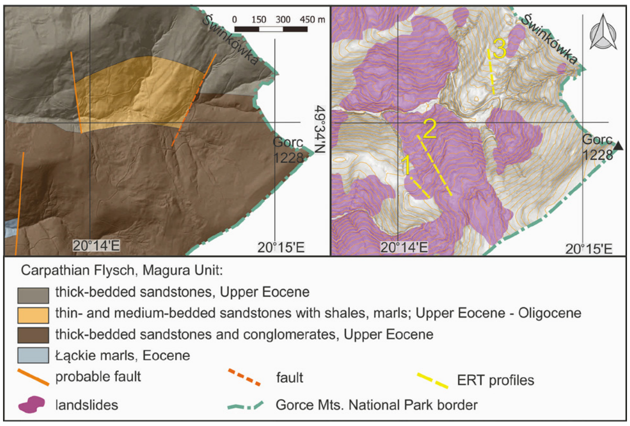

Fig. 2. Geology and relief of the study area. Geology units based on Cieszkowski et al. (2014)

(SOPO) by the Polish Geological Institute-National Research Institute (PIG-PIB). Between 2009 and 2012, all areas of Gorce municipalities outside the national park were mapped (Jurewicz et al. 2009, 2012, Konon et al. 2009; Lewandowski et al. 2010, Olszak, Kaczmarczyk 2011, Rubinkiewicz et al. 2012). The latest comprehensive study carried out within the park is the landslide occurrence map, which is the subject of this publication and was the element of the grant project funded by the Polish National Science Centre. Many researchers have studied the Gorce landslides in detail. Zbójecka Jama Cave in Jaworzyna Kamienicka was analyzed as an example of a tension crack being the initial stage of development of a landslide slope (Margielewski, Urban 2003). Wrońska (2006) and Wrońska-Wałach et al. (2013) drew attention to the important role of landslides in the formation of spring sinkholes. Lakes and peat bogs formed within the Gorce landslides are also a very important source of information about the natural history of this area. The sequence of sediments from Lake Iwanowskie (Bucała et al. 2014) in the Lubań range made it possible to determine the human impact on the environment in this area. Biogenic peat bog deposits at three sites in the Gorce Mountains have also been recently dated by Buczek (2019) and Kroh et al. (2021). Sediments from the Gorce ranges allowed for the collection of additional information on the development of the landslide landforms of the massif and climatic changes in the Gorce region in the Holocene. The mechanism of rockslide formation and the dating of landslide processes in the neighboring Beskid ranges (Beskid Sądecki, Wyspowy, and Średni) (Margielewski 2018, Kołaczek et al. 2020) have been identified very precisely thanks to thorough and long-lasting research. This research has allowed both the reconstruction of climate changes (Margielewski 2018) and analysis of the changes in the Carpathian flora during the Holocene (Bucała et al. 2014, Kołaczek et al. 2020). Thus, there is now a reference point for subsequent landslide studies in this part of the Carpathians. Geostatistical analyses of the national park area made it possible to determine the extent of landslides (Szczepanek et al. 2024), indicating the possibility of developing analyses based on a precise DEM.

Data and Methods

The methodology for landslide mapping over large areas still needs to be developed to ensure both effectiveness and reliability. This article is part of a larger project focused on mapping landslides throughout the entire Gorce Mountains National Park, which covers about half of the Gorce massif. The first step of this project was landslide mapping across the whole area of the national park based on DEM data. Subsequently, field verification, detailed mapping, and ERT profiles were conducted on smaller study sites that were unclear during DEM interpretation. The presented results are one element of a large-scale mapping focused more on identifying landslides than on understanding their mechanisms.

DEM analysis

The main material analyzed in this study is the DEM based on laser scanning performed in Poland as part of the construction of the IT system of the Country's Protection Against Extreme Hazards (ISOK). The input data for the DEMs was a point cloud produced *via* Airborne Laser Scanning (ALS). The scanning was done at a minimum density of 4 point*m-2 during the period of reduced vegetation (November to April) at a transversal scan angle of <= 25 degrees (Wężyk 2014). Filtering and classification of the point cloud were performed during post-processing, before the point cloud was delivered to the Head Office of Geodesy and Cartography. Therefore, the point cloud downloaded from governmental sources was already classified. The owner of the point cloud declares a classification accuracy of at least 95%. The DEM was generated at a resolution of 0.5 m in the Global Mapper 15 software, using the 'ground' class. This resolution was the highest level of detail that could be achieved given the available point cloud density.

The landslide vectorization was performed on a DEM-derived raster surfaces. These layers were: hillshade (angles: 45°, 135°, 225°, 315°), slope, Topographic Position Index (TPI) at three resolutions, Topographic Wetness Index (TWI) at three resolutions, total Sky View Factor (SVF), as well as negative and positive openness. The TPI and TWI coefficients were calculated using QGIS software, and the free Slovenian application was used to calculate SVF and openness (Zakšek et al. 2011, Kokalj et al. 2011).

After mapping landslides on the DEM, field verification was performed which consisted of checking the boundaries of the vectorized landslides, confirming their occurrence, and visualizing areas where landslides were not detected in the DEM. As a result of the field verification, areas with the greatest inconsistency between the DEM data and the landforms were identified. Consequently, these areas were accepted as research fields for further analysis and geophysical measurements. The geophysical measurements aimed to confirm or deny the existence of landslides in doubtful areas and to determine the extent of the occurrence. A hand-held Garmin 64s satellite navigation receiver able to read signals from two systems – GPS and GLONASS – and the mobile tMap software from TaxusIT, which enables vector mapping in the field based on the DEM and the geoposition, were used when mapping landslides.

ERT profiles were marked in three places:

Profile 1 was where the DEM showed no landslide, but field mapping indicated the occurrence of a shallow landslide.

Profile 2 went through a clearly occurring deep-seated landslide. This profile aimed to obtain information on how well the existing landslide was reproduced on the DEM – what landforms correspond to the situation below the surface.

Profile 3 was marked in an area whose relief is very difficult to interpret. Visual analysis of the DEM may indicate the occurrence of landslides; however, indicating the boundaries of potential landslides is a big problem.

Electrical resistivity tomography

Electrical resistivity tomography (ERT) was carried out using the LUND electrical imaging system with a Signal Averaging System (SAS) 4000 Terrameter produced by ABEM & Mala (Guideline Geo). The measuring system automatically measures the electrical resistivity values between individual electrodes along the profile line. The system consists of 41 electrodes and two cables with 21 takeouts and a maximum space of 5 m between electrodes. We conducted a roll-along survey to obtain profiles longer than 200 m. The distance between the electrodes was a = 5 m, and the Wen-ner-Schlumberger electrode configuration was used for all the profiles. This electrode array is moderately sensitive to both horizontal and vertical structures and has fairly good signal strength (signal-to-noise ratio) compared to other electrode configurations. The selected electrode spacing was chosen to provide a balance between the resolution of the near-surface layer and the depth of investigation, allowing the detection of structural heterogeneities within the landslide body while also achieving sufficient penetration to reach the expected slip surface at depth. The profile length was selected to cover the entire landslide zone from the crown to the toe, while also extending into stable ground beyond the margins of the unstable area, ensuring reliable resistivity contrasts. The achieved depth of investigation was primarily constrained by the maximum electrode spread of 200 m and the capabilities of the available measurement equipment, which limited the effective penetration to approximately 40 m, which is appropriate for characterizing the geometry and internal structure of medium to deep-seated landslides.

Three ERT profiles were carried out during the fieldwork on three landslides to confirm the landslides' geological formation. The lengths of the profiles were 300, 500, and 500 m for ERT1, ERT2, and ERT3, respectively. The electrode spacing made it possible to obtain the maximum penetration depth of approximately 40 m for all profiles.

The ERT data were processed and interpreted using RES2DINV (Geotomo Software). The program uses the smoothness-constrained Gauss-Newton least-squares inversion technique to determine a two-dimensional (2-D) resistivity model for the subsurface from the apparent resistivity data. The resulting model was based on 495, 952, and 963 measured points for ERT1, ERT2, and ERT3, respectively. The inversion was performed with the constrained least-squares formula, using an initial damping factor of 0.160 (minimum damping factor 0.015). The factor was increased with depth by a value of 1.05 and was not optimized for each iteration. A flatness filter was applied to the model perturbation vector, and the Jacobian matrix was recalculated for the first two iterations with a normal mesh. Forward modelling employed the finite-element method, and the inversion was carried out with an incomplete Gauss–Newton solution using a convergence limit of 0.005. The model cell width was set equal to the electrode spacing, with two nodes defined between adjacent electrodes. To incorporate the topography into the inversion model, we chose a distorted finite-element grid with damped distortion (damping factor = 0.75). The root-mean-squared (RMS) error, which describes the difference between the calculated and measured apparent resistivity values by adjusting the resistivity of the model blocks in each iteration process, was 4.5% (ERT1), 6.8% (ERT2), and 3.4% (ERT3), which indicates the rather good quality of the models but also the complexity of the landslide.

Landslide presence and depth were determined based on the most commonly accepted interpretation of resistivity results on ERT profiles worldwide. The sliding surface is almost always more humid than the landslide body. Additionally, the bedrock or slope material typically has a much denser structure compared to the landslide body, due to the mixed grain size distribution of the colluvium as a result of transport. Depending on the geological setting, typical ERT cross-sections of landslides are characterized by low electrical resistivity zones (usually from a few to several dozen m), indicating saturated or fine-grained material, and high electrical resistivity zones characterize solid, dry fractured bedrock or dry, coarse material. The transition zone corresponds to the slip surface marked as a concave upward, often dips gently downslope, and appears as a boundary between low and high resistivity electrical layers. These premises have allowed many researchers to interpret lower resistivity sections on the profile as the sliding surface (Bonetto et al. 2013, Masetti et al. 2013, Di Maio et al. 2016).

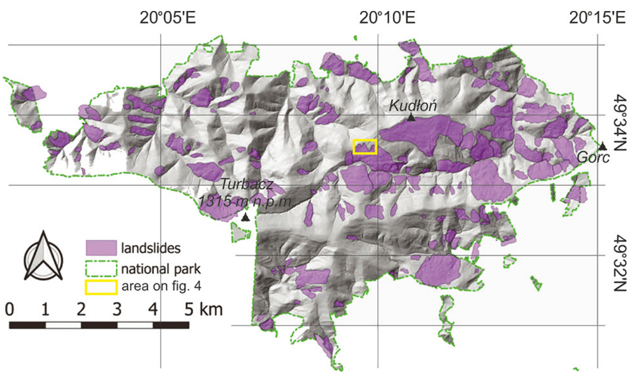

Fig. 3. Landslides in the Gorce National Park area. Delimitation of landslides by authors

Results

A total of 165 landslides were identified during the mapping of the entire National Park (Fig. 3). Most of them are inactive and can be recognized as stable landforms, with clearly visible niches and colluvial deposits. The majority are rock rotational slides, following the updated Varne's classification (Hungr et al. 2014), which is typical for the Polish Outer Carpathians within the Carpathian Flysch Belt. Many of these landslides have contributed to increased biodiversity, as the less steep and more humid conditions within landslide niches often support diverse forest associations, with a greater presence of habitats characteristic of stream source areas.

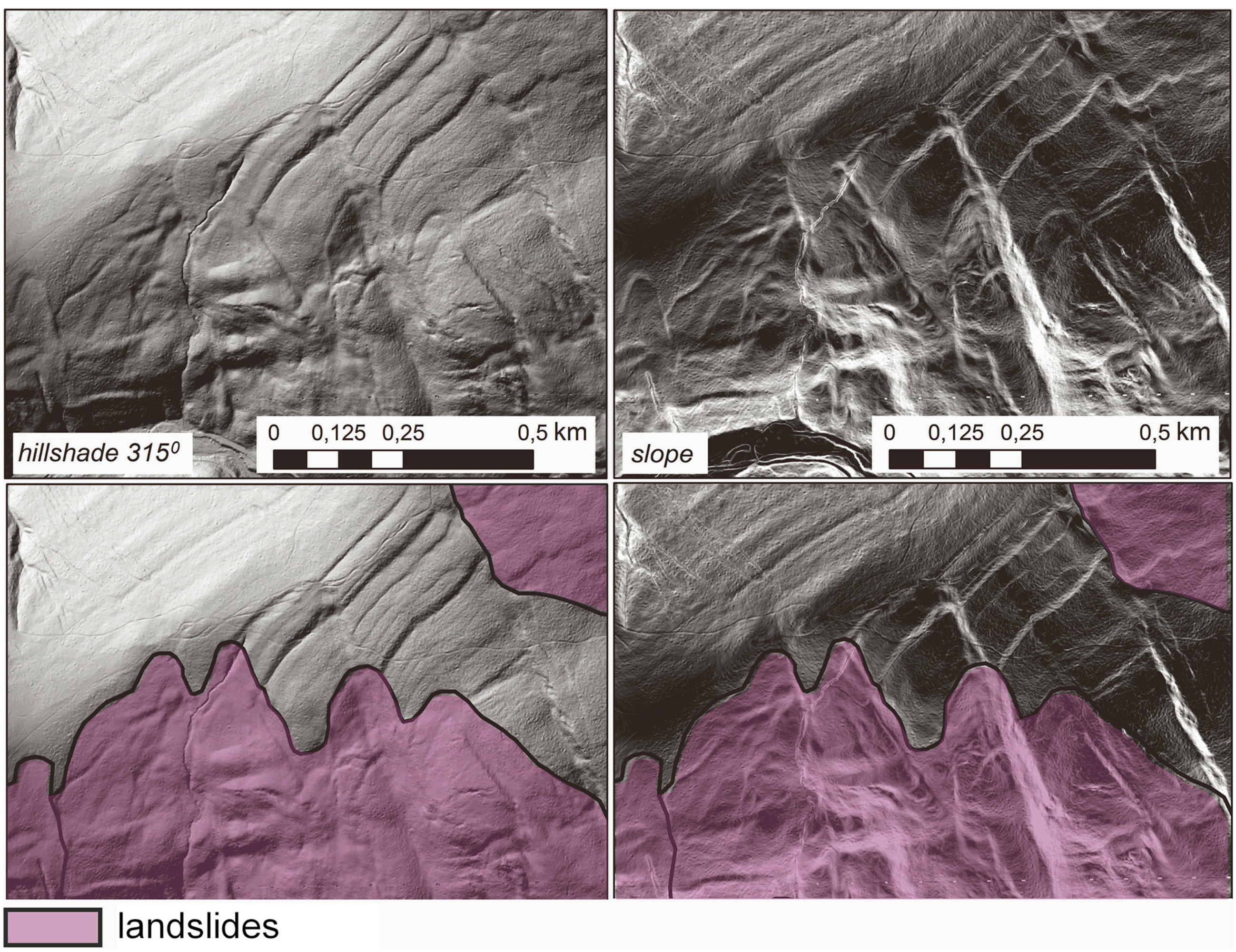

Fig. 4. Geological structure suggesting different landslide scarp delimitation

In some locations, visual interpretation of LiDAR-based DEM data proved to be unreliable. Therefore, field verification was conducted throughout the entire area. The most challenging areas for landslide delimitation were associated with three key factors:

- Locations where the geological structure was clearly visible in the high-resolution DEM, and its appearance could be misinterpreted as landslide scarps (Fig. 4);
- Slopes where surface relief-shaped by both geological structure and weathering were so spatially varied that they suggested the presence of colluvium, but without clearly defined niches above, interpreting potential landslide landforms was difficult (like in profile 3 below);
- Areas where landslide landforms are so extensive that they cover nearly the entire slope.

In three geomorphologically ambiguous terrain sites located in the eastern part of the massif, geophysical surveys were carried out to support landslide mapping and verify visual interpretations. Profiles 1 and 2 are situated on the northwestern slopes of Gorc Peak (1228 m a.s.l.), with landslides extending from approximately 1140 to 880 m a.s.l. Profile 3 is located on the southern slopes of the Świnkówka ridge, between 1080 and 930 m a.s.l. (Figs 1, 2).

Profile 1

The landslide was identified during field mapping. Analysis of the DEM (hill-shade 45, 135, 225, 315; slope, TWI, TPI (2, 10, and 33 m), positive and negative openness, SVF) was performed, but none of these raster versions showed the occurrence of a landslide. It was mapped during field mapping as a shallow weathering landslide. Conflicting data from the field and model analyses prompted the question "is there a landslide?" and the selection of this place for an ERT1 profile (Fig. 5).

ERT shows the occurrence of a shallow landslide. The lower resistivity values (11–115 Ωm), constituting one spatial whole from 30 m to 250 m of the profile, correspond to the boundaries mapped in the field. The increase in surface resistivity (above 115 Ωm) at around 130 m of the profile is related to the course of the road, which cuts into the slope and additionally retains surface water. However, the decrease in resistivity recorded between 135 m and 175 m (11-115 Ωm) is related to the occurrence of increased humidity of the surface formations. A sharp change in resistivity at a depth of approximately 4–5 m below ground level indicates the sliding surface, which separates the displaced soil masses from the more heterogeneous bedrock. The bedrock includes sandstone layers, visible as three sections with resistivity values above 530 Ωm. A significant increase in resistivity from 255 m indicates leaving the landslide area and moving to the lower part of the profile on rock formations that were cut by a stream. ERT confirms the thesis that not all landslides are visible in DEMs, even if various raster backgrounds are interpreted.

Shallow, slow-moving landslides are often associated with changes in vegetation cover. In this case, however, vegetation is not a factor influencing the process. The area belongs to the strict protection zone of the national park, where no forestry management is carried out. The forest structure consists of beech (60%), spruce (30%), and fir (10%), with an average age of 110 years. The trees are sparsely distributed, and in the lower forest layer, natural regeneration (mostly beech) covers about 10% of the area. Such vegetation structure is neutral for shallow landslides in the Flysch Carpathians – it does not increase landslide susceptibility, but it also does not strongly stabilize the upper soil layers.

Profile 2

Profile 2 was conducted through a deep-seated landslide, which is very clear to identify on the DEM. The main scarp is very clear, regardless of the analyzed raster background. All formations are easily recognizable, showing a large landslide and three scarps occurring within them (Fig. 6).

The ERT profile was planned in such a way that it ran through two distinct landslide scarps and also included the lower part of the colluvium. The profile

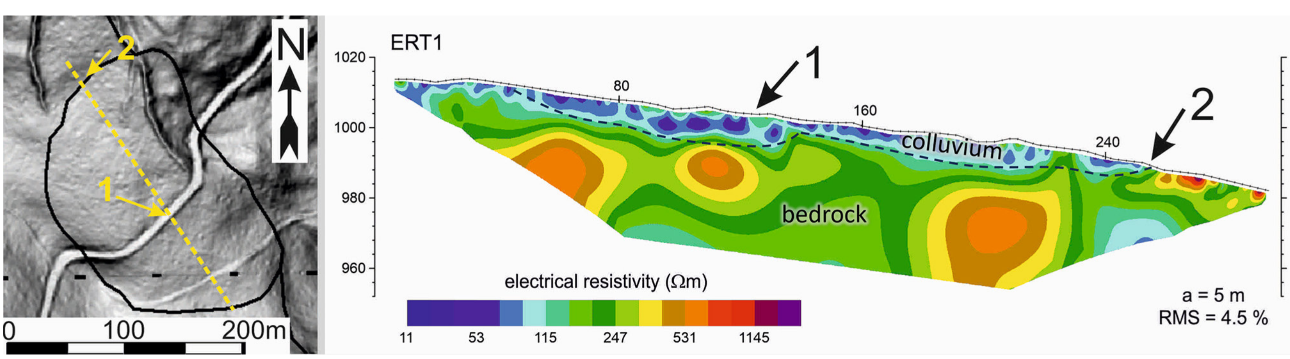

Fig. 5. Inversion results of ERT measurements of profile ERT1 and DEM of landslide 1

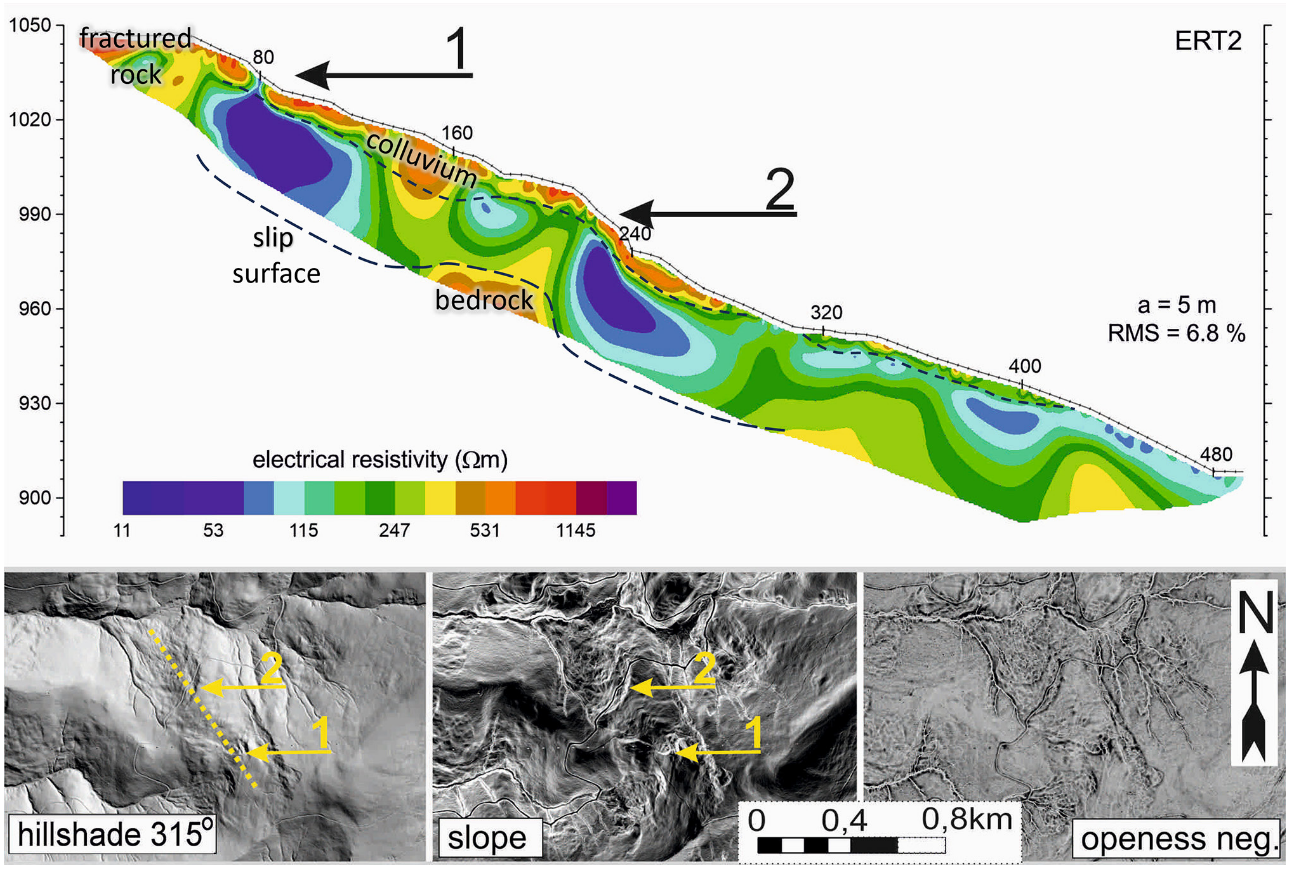

Fig. 6. Inversion results of ERT measurements of profile ERT2 and DEM on three different terrain images

aimed to determine whether individual fragments of the scarp constitute one large landslide, within the boundaries of which a secondary scarp was formed, or whether these are genetically independent forms. Obtaining such information would enable the interpretation of the DEM in terms of landform features indicating the above-mentioned genesis.

Both landslide scarps are clearly marked by a very strong reduction in resistivity on the ERT profile (around 53 Ωm). This reduction also shows the course of the main sliding surface, which classifies them as rotational landslides according to Varne's classification (Hungr et al. 2014). The location of the resistivity reduction corresponds to the location of the landslide scarps in the field and on the DEM. Unfortunately, the landslide turned out to be much deeper than researchers expected. The depth of the ERT profile exceeded 40 m and proved to be insufficient for providing a clear answer to the question of whether it was one or two landslides. A significantly different shape of the course and a smaller depth of the layer of lower resistivity in the area of the lower scarp would suggest the occurrence of one landslide with secondary displacement. This concept is also confirmed by a distinct layer of reduced resistivity at a depth of approximately 10 m in the lower part of the colluvium. The section with the highest resistivity (marked in red, above 600 Ωm) indicates areas with an accumulation of sandstone blocks above and below the main scarp. The section beyond 300 m of the profile shows diverse resistivity with generally low values (~50–250 Ωm), which corresponds to mixed colluvial deposits containing a high proportion of sandy-clay material.

These results indicate that the visual analysis of the DEM is highly correct. Determining the boundaries of the landslide, landslide scarps, and the extent of the colluvium in the case of deep-seated landslides is not very difficult and is characterized by a low probability of error.

Profile 3

The third research site was chosen owing to the very ambiguous image of the area. At the stage of visual interpretation, three versions of "landslides" on this slope were created, and all three seemed probable to the authors. Three DEM transformations are presented in Figure 7. Field mapping only partially clarified the picture – it indicated areas where landslides were impossible. The interpretation of landforms was so ambiguous that it was decided to conduct an ERT profile.

The ERT method confirmed the absence of landslides on Profile 3. The zones of reduced electrical resistivity (below 531 Ωm), clearly occurring at 160,

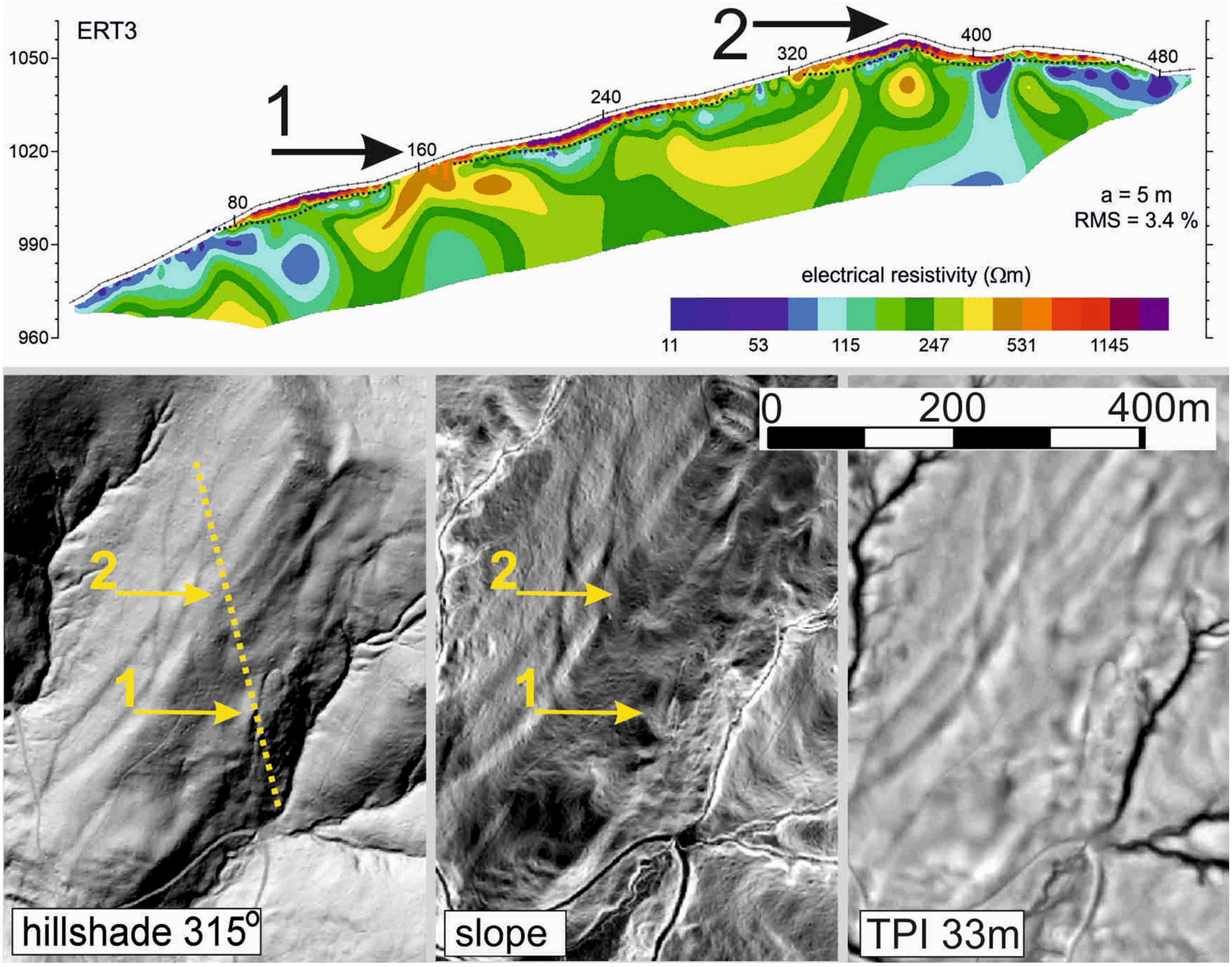

Fig. 7. Inversion results of ERT measurements of profile ERT3 and DEM on three different terrain images

305, and 415 m, indicate that they are not a landslide sliding surface. The regularity suggests the presence of rock layers of higher density or moisture on the surface, probably shale interlayers between sandstones, which are typical in flysch areas. The lower part of the profile, which is a large fraction of debris formation, is not a colluvium, but a specifically weathered geological layer. This is evidenced by its arrangement relative to the slope, the lack of a sliding surface on the ERT profile, and the lack of landform features that would indicate landslides in this part of the area. The zones with the highest resistivity values (red, exceeding ~800 Ωm) indicate the presence of block-weathered sandstone. The deep, vertically running zone with a reduction in resistivity at 415 m of the profile is probably a small, unrecognized fault. This could also be related to a larger fault shown on geological maps (Fig. 2) located in close proximity to this profile. The low resistivity of the end of the profile (below 53 Ωm) is related to the spring sinkhole, strong substrate moisture, and the spring zone of the stream.

Discussion

Visual interpretation of DEMs is still the most frequently used method for quick and large-scale mapping of landslides, although the first applications of these methods were implemented almost two decades ago (Eeckhaut et al. 2007, Jaboyedoff 2012). The Gorce Mountains exhibit a wide spectrum of landslide ages (Buczek 2015, Buczek 2019, Kroh et al. 2021). Most of them, however, can be classified as "old," following the understanding of landforms introduced by the first advanced research using LiDAR in landslide mapping (Eeckhaut et al. 2007). Our research once again clearly confirms the usefulness of this tool. The lack of strict delimitation criteria and the intuitive nature of the method mean that visual landslide mapping on high-precision DEMs is fast and – paradoxically, despite the absence of clear criteria – highly accurate. LiDAR techniques are highly effective for detecting all types of land surface deformations, allowing both shallow and deep-seated landslides to be mapped with these methods (Jaboyedoff 2012). By comparing the effectiveness of DEM visual interpretations from the early days of LiDAR usage, readers can see that the experience gained by researchers worldwide over the past two decades – combined with the development of GIS techniques, such as the common use of TPI, TWI, openness, or SVF indexes in raster transformations – has led to expert visual interpretations that are now far more accurate than those achieved in the early 2000s (Eeckhaut et al. 2007, Kroh et al. 2014).

These can be particularly effective in determining landslide areas for spatial planning purposes. They also enable the identification of questionable areas, potentially at risk of slippage and landslides, by noticing fragments of slopes where the slope morphology differs from the neighboring slopes.

Differences between digital mapping on the DEM and the field corrected results at the scale of the entire national park were surprisingly small. Only one small shallow landslide was missed on the DEM (which became the study site with Profile 1 described in this paper). One part of the slope was initially vectorised as a landslide, although it did not represent a true landslide, which was later designated as Profile 3. A clearly visible geological structure caused some confusion but did not lead to mapping errors. Other corrections made after the fieldwork involved splitting one landform into two, but within almost the same boundaries (Table 1).

However, it must be remembered that the interpretation of DEMs is not as easy and unambiguous as it seems at first glance. Despite the use of precise raster material and extensive experience in mapping landslides, the DEM failed to detect a shallow landslide, which subsequently became the subject of research on Profile 1. The ERT method confirmed the existence of the landslide, thereby verifying the incorrect interpretation of the DEM and the accuracy of the terrain mapping.

The same thing happened for Profile 3. The "initial vectorisation" interpretation of the model turned out to be completely wrong. However, it pointed to a place that is difficult to interpret. Thanks to this, field verification and re-mapping were carried out. Field interpretation and a more detailed analysis of a fragment of the model allowed for a more correct delimitation of the landslide boundaries in this area. ERT confirmed the absence of a landslide, that is, the correct interpretation made "in the second mapping" after field verification.

Correct visual mapping of landslides requires following certain procedures. The interpretation of the DEM is not as clear as it seems at first glance. The very high plasticity of DEMs seems very easy. According to the authors, to correctly interpret the DEM in terms of landslides, each vectorized fragment should be analyzed on backgrounds such as hillshade illuminated from four angles, slope, aspect, SVF, and TPI.

Table 1. Mistakes or difficulties in DTM interpretation met during landslide mapping in Gorce National Park

Mistakes or difficulties in DEM interpretation	Reason of missinterpretations	How to avoid	ERT role
False negative interpretation (missing shallow landslide)	Only surface movement; poorly visible landform in the field and on the DEM.	DEM interpretation should be done by a researcher with field mapping experience. This increases the chance of proper delimitation in ambiguous areas and helps identify places for field verification.	Confirms or excludes the presence of a landslide.
False positive interpretation (slope morphology treated as landslide)	Landslide slopes often have undulating microrelief in Carpathian flysch regions. Non-landslide slopes with similar relief (rare) can appear as landslides on the DEM.	Identify the main scarp and colluvium range on the DEM. If clear delineation is not possible, mark the area for field verification.	Confirms or excludes the presence of a landslide.
Improper delineation of landforms within larger landslide areas (mapping separate landslides as one landform)	Initial vectorization was done on slope, openness, and hillshade rasters in grayscale. These showed the presence of a landslide, so the entire area with landslide relief was mapped as a single landform.	Conduct a more detailed analysis using different DEM rasters, including aspect maps in color. Analyze additional topographic elements (e.g., stream network).	ERT usually not necessary.
Geological structure misinterpreted as landslide scarp	A geological structure visible on the DEM often resembles a resistant layer, which can look similar to a landslide scarp.	Landslide scarps are usually less regular than geological structures. Geological layers often continue through the mountain range with the same orientation in valleys and ridges.	A more detailed DEM analysis is usually sufficient. ERT confirms or excludes the presence of a landslide.

Analyzing only the hillshade model, which is most available on, for example, government geoportals, may lead to very serious errors. Additionally, it is necessary to interpret the model at least twice. Landslides vectorized "at the initial vectorisation" should be verified by another researcher, or by the same one, but after a long break (from the authors' experience, it should be at least week or two) after vectorization. Questionable places should also be identified and verified in the field.

The resolution of the DEM can also influence the detail of landslide mapping. Too low resolution may cause smaller landslides to be missed. In our case, this is not a significant problem. A 0.5 m resolution at both the whole massive and slope scales provides confidence that even very small landslides will not be omitted. We generated the DEM from the point cloud ourselves to control all parameters used in its creation. Comparing our DEM with those available on the official governmental geoportal, we conclude that, at our scale of research, the difference between 0.5 m (our DEM) and 1 m (governmental data) resolution would not affect the precision of landslide mapping.

Limitations and errors of the ERT method could be described at measurement stage, inversion process and at interpretation stage. The difficulty of the complicated terrain of the landslide can be a source of poor electrode grounding, causing data quality problems and data gaps. The solution for improving the electrode contact can be, e.g., watering or possibly connecting several electrodes to each electrode point. Uncertainties connected with the ERT method can also be caused by the wrong cable connection and coupling between the cables, which are sources of systematic errors (ABEM 2018).

The measurement parameters, such as electrode spacing and profile length, which correspond with the maximum depth range, and the resolution of the near-surface layer, should be aligned with the landslide characterization. The selection of the array configuration type can also impact the shape of the anomalies visualized in the model. However, the most common array configuration used for landslides is Wenner-Schlumberger due to its moderate sensitivity to horizontal and vertical structures, better horizontal coverage, and good signal strength compared to other arrays (Loke 2004).

During the interpretation stage, a small contrast between the landslide body and bedrock can cause problems in accurately delineating the exact location of the sliding surface. A similar effect can be caused by the low resolution of the ERT measurements. The non-uniqueness of the inversion model related to the range of models created based on the same calculated apparent resistivity values in the landslide application is emphasized by the variation of the structure of the material (including rock, debris, soil, or their combination), including the geological structures like faults, high groundwater levels, and fractured bedrock, displacement, and strain. The non-uniqueness can be reduced by the assumptions concerning the nature of the sub-surface from maps and boreholes of the surrounding area, other geotechnical surveys, and geodetic measurements, and incorporated into the inversion subroutine (Olabode et al. 2022).

Geophysical methods are time-consuming, both during data acquisition and due to the need for transporting heavy equipment to remote locations; however, the results they provide are highly reliable. A main scarp (a steep slope break or a crown) on the DEM may correspond in ERT to a near-surface high electrical resistivity zone interpreted as relatively dry and competent materials such as debris or shallow bedrock transitioning into a lower electrical resistivity layer beneath, indicating a potential shear zone or failure surface. The toe of the landslide, characterized in the DEM by an abrupt convex break or accumulation, often corresponds to low resistivity zones in ERT, suggestive of saturated or poorly compacted materials, which is a common feature in colluvial deposits. Meanwhile, concave-upward electrical resistivity boundaries in ERT, dipping downslope, often align with subsurface failure planes. These zones also intersect features like midslope benches or internal scarps visible in DEM (Luhn et al. 2023, Bhuyan et al. 2025). Many landslide studies have shown that electrical resistivity is an effective parameter for clearly detecting discontinuities in bedrock and soil materials. Identification of the sliding surface using the ERT method is reliable. Consequently, detecting the presence, extent, and boundaries of landslides with ERT can effectively verify DEM data. When ERT is applied to confirm the delimitation of landslide boundaries in ambiguous areas, it offers a robust and dependable solution. ERT clearly supported one of the DEM interpretation hypotheses and provided definitive evidence either confirming or refuting the presence of a landslide in specific locations.

This study demonstrates that high-resolution, LiDAR-based DEMs are excellent tools for the general delineation of landslide areas, particularly for applications such as assessing landslide susceptibility for spatial planning purposes. Nevertheless, they may be insufficient when a highly precise determination of mass movement extents on slopes is required. Taking potential interpretation difficulties into account, visual analysis of high-precision LiDAR DEMs currently remains the most efficient method for landslide mapping, especially in remote areas densely covered by vegetation.

Conclusions

High-resolution DEMs have been used for landslide mapping for more than two decades. Visual interpretation of DEMs is still the most widely used and effective method of landslide mapping. LiDAR-based DEMs are already so precise that higher data resolution will not improve landslide mapping, making methodological improvement necessary.

Deep-seated landslides are very clearly visible on precise DEMs. Determining their boundaries is unambiguous, and the analysis of various DEM processing allows for the precise determination of the boundaries of landslide scarps. In turn, shallow landslides may be difficult to interpret and, even with very high-resolution DEMs, sometimes impossible to identify only on a computer screen.

The geophysical ERT method proved to be very effective for point-by-point verification of the results obtained as part of multi-site landslide mapping. Preparing ERT profiles in places that raise doubts in interpretation is a very good tool for verifying the extent of landslides and confirming or denying their occurrence.

This study also shows that even the most precise data obtained remotely do not enable full interpretation of the geoenvironment, and field studies, both geomorphological and interdisciplinary, are still necessary to accurately determine the occurrence of landslides.

Acknowledgements

This research was funded by the Polish National Science Center, grant number 370834. The authors would like to thank the reviewers for their helpful suggestions to improve this article.

Author Contributions

P.K.: Conceptualization, methodology, field investigation, writing-original draft preparation, writing-review and editing; M.K.: methodology, field investigation, writing-original draft preparation; D.I.: field investigation,

References

ABEM, 2018. Terrameter SAS 4000/SAS 1000, User Manual.

Abu-Shariah M.I.I., 2009. Determination of Cave Geometry by Using a Geoelectrical Resistivity Inverse Model. Engineering Geology 105: 239–244. DOI: 10.1016/j.enggeo.2009.02.006.

Batayneh A., Al-Diabat A., 2002. Application of a Two-Dimensional Electrical Tomography Technique for Investigating Landslides along the Amman-Dead Sea Highway, Jordan. Environmental Geology 42: 399–403. DOI: 10.1007/s00254-002-0543-x.

Bhuyan K., Rana K., Ozturk U., Nava L., Rosi A., Meena S.R., Fan X., Floris M., van Westen C., Catani F., 2025.Towards automatic delineation of landslide source and runout. Engineering Geology 345: 107866. DOI: 10.1016/J.ENGGEO.2024.107866.

Bichler A., Bobrowsky P., Best M., Douma M., Hunter J., Calvert T., Burns R., 2004. Three-Dimensional Mapping of a Landslide Using a Multi-Geophysical Approach: The Quesnel Forks Landslide. Landslides 1: 29–40. DOI: 10.1007/s10346-003-0008-7.

Bonetto S., Comina C., Giuliani A., Mandrone G., 2013. Geological and Geophysical Tests to Model a Small Landslide in the Langhe Hills. In: Margottini C., Canuti P., Sassa K. (eds), Landslide Science and Practice; Springer Berlin Heidelberg: Berlin, Heidelberg: 95–101.

Bucała A., Margielewski W., Starkel L., Buczek K., Zernitskaya V., 2014. The Reflection of Human Activity in the Sediments of Iwankowskie Lake from Subatlantic Phase (Polish Outer Carpathians). Geochronometria 41: 377–391. DOI: 10.2478/s13386-013-0172-z.

Bucała A., Budek A., Kozak M., Starkel L., Wiejaczka Ł., 2016. Kierunki przemian środowiska przyrodniczego dolin gorczańskich. Prace Geograficzne (252): 1–113.

Buczek K., 2015. Wpływ działalności człowieka na funkcjonowanie jeziora osuwiskowego, na przykładzie Pucołowskiego Stawku w Gorcach. Prace Geograficzne (142): 41-56. DOI: 10.4467/20833113PG.15.017.4457.

Buczek K., 2019. Dating Landslides in the Gorce Mts. (Polish Outer Carpathians) – Preliminary Results. Geological Quarterly 63: 849-860. DOI: 10.7306/gq.1501.

Cebulski J., Pasierb B., Wieczorek D., Zieliński A., 2020. Reconstruction of landslide movements using Digital Elevation Model and Electrical Resistivity Tomography analysis in the Polish Outer Carpathians. Catena 195: 104758. DOI: 10.1016/j.catena.2020.104758.

Cieszkowski M., Szczęch M., Chodyń R., 2014. Mapa geologiczna odkryta Gorczańskiego Parku Narodowego. Usługi Ekologiczne (unpubl. documentation).

Di Maio C., Scaringi G, Vassallo R., Rizzo E., Perrone A., 2016. Pore Fluid Composition in a Clayey Landslide of Marine Origin and Its Influence on Shear Strength along the Slip Surface. In: Aversa S., Cascini L., Picarelli L., Scavia C. (eds), Landslides and Engineered Slopes. Experience, Theory and Practice; CRC Press, 813–820.

Dolžan E., Jemec Auflič M., 2017. Using Lidar DEM to Map Landslides: Škofjeloško Cerkljansko Hills, Slovenia. In: Mikos M., Tiwari B., Yin Y., Sassa K. (eds), Advancing Culture of Living with Landslides; Springer International Publishing: Cham: 191–199. DOI: 10.1007/978-3-319-53498-5_22.

Đomlija P., Bernat S., Arbanas Mihalić S., Benac Č., 2014. Landslide Inventory in the Area of Dubračina River Basin (Croatia). In: Sassa K., Canuti P., Yin Y. (eds), Landslide Science for a Safer Geoenvironment; Springer International Publishing: Cham: 837–842.

Drahor M.G., Göktürkler G., Berge M.A., Kurtulmuş T.Ö., 2006. Application of Electrical Resistivity Tomography Technique for Investigation of Landslides: A Case from Turkey. Environmental Geology 50: 147–155, DOI: 10.1007/s00254-006-0194-4.

Eeckhaut M. Van Den, Poesen J., Verstraeten G., Vanacker V., Nyssen J., Moeyersons J., Beek L.P.H. van, Van-Dekerckhove L., 2007. Use of LIDAR-derived Images for Mapping Old Landslides under Forest. Earth Surface Processes and Landforms 32: 754–769, DOI: 10.1002/esp.1417.

Forma A., Zuchiewicz W., 2002. Morphotectonics of the Gorce Mountains, Western Outer Carpathians. Folia Quaternaria 73: 69–78.

Gerlach T., 1976. Współczesny rozwój stoków w Polskich Karpatach Fliszowych. Prace Geograficzne 122: 1–128.

Gorum T., Fan X., van Westen C.J., Huang, R.Q., Xu Q., Tang C., Wang G., 2011. Distribution Pattern of Earthquake-Induced Landslides Triggered by the 12 May 2008 Wenchuan Earthquake. Geomorphology 133: 152–167. DOI: 10.1016/j.geomorph.2010.12.030.

Grabowski D., Przybycin A., 2010. Z działalności administracji geologicznej Działania resortu środowiska w zakresie systemu osłony przeciwosuwiskowej w Polsce.Przegląd Geologiczny 58(10): 941-945.

Hungr O., Leroueil S., Picarelli L., 2014. The Varnes classification of landslide types, an update. Landslides 11:167–194. DOI: 10.1007/s10346-013-0436-y.

Jaboyedoff M., Oppikofer T., Abellán A., Derron M.-H., Loye A., Metzger R., Pedrazzini A., 2012. Use of LIDAR in Landslide Investigations: A Review. Natural Hazards 61: 5–28. DOI: 10.1007/s11069-010-9634-2.

Jomard H., Lebourg T., Tric E., 2007. Identification of the Gravitational Boundary in Weathered Gneiss by Geophysical Survey: La Clapière Landslide (France). Journal of Applied Geophysics 62: 47–57. DOI: 10.1016/j.jappgeo.2006.07.003.

Jurewicz E., Kaczorowski J. Klimkiewicz D., Konon A., Ludwiniak M., Ozimkowski W., Rubinkiewicz J., Sobstyl A., Śmigielski M., Tomaszczyk M., 2009. Mapa Osuwisk i Terenów Zagrożonych Ruchami Masowymi w Skali 1:10000, Gm. Mszana Dolna.

Jurewicz E., Ozimkowski W., Rubinkiewicz J., Śmigielski M., Tomaszczyk M., Cybulska D., Stachowska A., Stępczak P., 2012. Mapa Osuwisk i Terenów Zagrożonych Ruchami Masowymi w Skali 1:10000, Gm. Ochotnica Dolna.

Kasprzak M., Duszyński F., Jancewicz K., Michniewicz A., Różycka M., Migoń P., 2016. The Rogowiec Landslide Complex (Central Sudetes, SW Poland) – a case of a collapsed mountain. Geological Quarterly 60(3):227–242. DOI: 10.7306/gq.1286.

Kasprzak M., Jancewicz K., Różycka M., Kotwicka W., Migoń P., 2019. Geomorphology- and geophysics-based recognition of stages of deep-seated slope deformation (Sudetes, SW Poland). Engineering Geology 260: 105230. DOI: 10.1016/j.enggeo.2019.105230.

Klimaszewski M., Starkel L., 1972. Karpaty Polskie, In: Klimaszewski M. (ed), Geomorfologia Polski, t.1., PWN, Warszawa: 21-115.

Kokalj Ž., Zakšek K., Oštir K., 2011. Application of Sky-View Factor for the Visualisation of Historic Landscape Features in Lidar-Derived Relief Models. Antiquity 85: 263–273. DOI: 10.1017/S0003598X00067594.

Kołaczek P., Margielewski W., Gałka M., Karpińska-Kołaczek M., Buczek K., Lamentowicz M., Borek A., Zernitskaya V., Marcisz K., 2020. Towards the Understanding the Impact of Fire on the Lower Montane Forest in the Polish Western Carpathians during the Holocene. Quaternary Science Review 229 106137, DOI: 10.1016/j.quascirev.2019.106137.

Konon A., Rubinkiewicz J., Śmigielski M., Klimkiewicz D., Tomaszczyk M., 2009. Mapa Osuwisk i Terenów Zagrożonych Ruchami Masowymi w Skali 1:10000, Gm. Niedźwiedź.

Kroh P., 2017. Analysis of Land Use in Landslide Affected Areas along the Łososina Dolna Commune, the Outer Carpathians, Poland. Geomatics, Natural Hazards and Risk 8: 863–875. DOI: 10.1080/19475705.2016.1271833.

Kroh P., Okupny D., Bryndal T., Kondracka M., Cybul P., 2021. Holoceńskie Okresy Intensyfikacji Procesów Stokowych w Gorcach – Porównanie Najnowszych Wyników Badań. Przegląd Geograficzny 93: 83–101. DOI: 10.7163/PrzG.2021.1.5.

Kroh P., Pawlik Ł., 2021. Recent Advances on Geomorphology of the Gorce Mountains, the Outer Western Carpathians – State-of-the-Art and Future Perspectives. Geographia Polonica 94: 47–67. DOI: 10.7163/GPol.0193.

Kroh P., Struś P., Gorczyca E., Wrońska-Wałach D., Długosz M., 2014. Identification of Landslides in Łososina Dolna Commune Based on Spatial Data from Airborne Laser Scanning. Problemy Ekologii Krajobrazu 38: 61–75.

Kroh P., Struś P., Wrońska-Wałach D., Gorczyca E., 2019. Map of landslides on the commune scale based on spatial data from airborne laser scanning. Carpathian Journal of Earth and Environmental Sciences 14(1): 155-164. DOI: 10.26471/cjees/2019/014/067.

Lapenna V., Lorenzo P., Perrone A., Piscitelli S., Sdao F., Rizzo E., 2003. High-Resolution Geoelectrical Tomographies in the Study of Giarrossa Landslide (Southern Italy). Bulletin of Engineering Geology and the Environment 62: 259–268. DOI: 10.1007/s10064-002-0184-z.

Lapenna V., Perrone A., 2022. Time-Lapse Electrical Resistivity Tomography (TL-ERT) for Landslide Monitoring: Recent Advances and Future Directions. Applied Sciences 12: 1425, DOI:10.3390/app12031425.

Leopold P., Tao W., Perko R., Heiss G., Jung M., Oblin A., Zhang Y., 2017. Comparing Landslide Mapping from DEM Satellite Derived Data and Field Based Studies of Loess Sediments in Western China. In: Mikos M., Tiwari B., Yin Y., Sassa K. (eds), Advancing Culture of Living with Landslides; Springer International Publishing: Cham: 87–95.

Lewandowski J., Wojciechowski T., Salomon T., 2010. Mapa Osuwisk i Terenów Zagrożonych Ruchami Masowymi w skali 1:10000, Gm. Rabka-Zdrój.

Loke M.H., 2004. Res2Dinv v. 3.54 for Windows 98/Me/2000/NT/XP. Rapid 2D Resistivity and IP Inversion Using the Least-Squares Method. Software Manual.

Luhn J., Stumvoll-Schmaltz M.J., Orozco A.F., Glade T., 2023. The internal structure of an active landslide based on ERT and DP data: New insights from the Hofermühle landslide observatory in Lower Austria. Geomorphology 441: 108910. DOI: 10.1016/J.GEOMORPH.2023.108910.

Marciniak A., Kowalczyk S., Gontar T., Owoc B., Majdański M., 2021. Integrated geophysical imaging of a mountain landslide: A case study from the Outer Carpathians, Poland. Journal of Applied Geophysics 191: 104364. DOI: 10.1016/j.jappgeo.2021.104364.

Margielewski W., 2018., Landslide Fens as a Sensitive Indicator of Paleoenvironmental Changes Since the Late Glacial: A Case Study of the Polish Western Carpathians. Radiocarbon 60: 1199–1213. DOI: 10.1017/RDC.2018.68.

Margielewski W., 1998. Landslide Phases in the Polish Outer Carpathians and Their Relation to Climatic Changes in the Late Glacial and the Holocene. Quaternary Studies in Poland 15: 37–53.

Margielewski W., Urban J., 2003. Crevice-Type Caves as Initial Forms of Rock Landslide Development in the Flysch Carpathians. Geomorphology 54: 325–338. DOI: 10.1016/S0169-555X(02)00375-6.

Masetti G., Ottria G., Ghiselli F., Ambrogio A., Rossi G., Zanolini L., 2013. Multidisciplinary Study of the Torrio Landslide (Northern Apennines, Italy). In: Margottini C., Canuti P., Sassa K. (eds), Landslide Science and Practice; Springer Berlin Heidelberg: Berlin, Heidelberg: 177–184. DOI: 10.1007/978-3-642-31325-7_23.

Migoń P., Jancewicz K., Różycka M., Duszyński F., Kasprzak M., 2017. Large-scale slope remodelling by landslides – geomorphic diversity and geological controls, Kamienne Mts, Central Europe. Geomorphology 289: 134–151. DOI: 10.1016/j.geomorph.2016.09.037.

Niemirowski M. ,1974. Dynamika współczesnych koryt potoków górskich (na przykładzie potoków Jaszcze i Jamne w Gorcach). Zeszyty Naukowe UJ, Prace Geograficzne 34: 1–105.

Obrębska-Starklowa B., 1969. Mezoklimat zlewni potoków Jaszcze i Jamne, Studia Naturae Ser. A 3: 1–102.

Olabode O.P., Lim H.S., Ramli M.H., 2022. Geophysical and Geotechnical Evaluation of Landslide Slip Surface in a Residual Soil for Monitoring of Slope Instability. Earth and Space Science 9(12) e2022EA002248. DOI: 10.1029/2022ea002248.

Olszak J., Kaczmarczyk R., 2011. Mapa Osuwisk i Terenów Zagrożonych Ruchami Masowymi w skali 1:10000, Gm. Kamienica.

Oszczypko N., Oszczypko-Clowes M., 2012. Stages of Development in the Polish Carpathian Foredeep Basin. Open Geosciences 4: 138-162. DOI: 10.2478/s13533-011-0044-0.

Pánek T., Margielewski W., Tábořík P., Urban J., Hradecký J., Szura C., 2010. Gravitationally Induced Caves and Other Discontinuities Detected by 2D Electrical Resistivity Tomography: Case Studies from the Polish Flysch Carpathians. Geomorphology 123: 165–180. DOI: 10.1016/j.geomorph.2010.07.008.

Rubinkiewicz J., Karwacki K., Kwecko P., 2012. Mapa Osuwisk i Terenów Zagrożonych Ruchami Masowymi w skali 1:10000, Gm. Nowy Targ.

Samodra G., Ramadhan M.F., Sartohadi J., Setiawan M.A., Christanto N., Sukmawijaya A., 2020. Characterization of Displacement and Internal Structure of Landslides from Multitemporal UAV and ERT Imaging. Landslides 17: 2455–2468. DOI: 10.1007/s10346-020-01428-0.

Sass O., Bell R., Glade T., 2008. Comparison of GPR, 2D-Resistivity and Traditional Techniques for the Subsurface Exploration of the Öschingen Landslide, Swabian Alb (Germany). Geomorphology 93(1-2): 89–103. DOI: 10.1016/j.geomorph.2006.12.019.

Schrott L., Sass O., 2008. Application of Field Geophysics in Geomorphology: Advances and Limitations Exemplified by Case Studies. Geomorphology 93: 55–73. DOI: 10.1016/j.geomorph.2006.12.024.

Sigdel A., Adhikari R.K., 2020. Application of Electrical Resistivity Tomography (ERT) Survey for Investigation of the Landslide: A Case Study from Taprang Landslide, Kaski District, West-Central Nepal. Journal of Nepal Geological Society 60: 103–115. DOI: 10.3126/jngs.v60i0.31261.

Solon J., Borzyszkowski J., Bidłasik M., Richling A., Badora K., Balon J., Brzezińska-Wójcik T., Chabudziński Ł., Dobrowolski R., Grzegorczyk I., et al., 2018. Physico-Geographical Mesoregions of Poland: Verification and Adjustment of Bounda-ries on the Basis of Contemporary Spatial Data. Geographia Polonica 91: 143–170. DOI: 10.7163/GPol.0115.

Suhendra S., Sinaga J.E.E., Fadli D.I., Halauddin H., Supiyati S., 2024. 2D and 3D Modelling Electrical Resistivity Tomography (ERT) of Landslide Sliding and Weak Bedding Plane Along Mountain Road North Bengkulu-Lebong, Indonesia. Geosfera Indonesia 9(1): 29-40. DOI: 10.19184/geosi.v9i1.38065.

Sun M., Liu J., Ou J., Liu R., Zhu L., 2024. Electrical Resistivity Tomography (ERT) Investigation for Landslides: Case Study in the Hunan Province, China. Applied Sciences 14: 3007. DOI: 10.3390/app14073007.

Szczepanek R., Szczęch M., Kania M., 2024. Landslide Type Inference Based on Statistical Analysis of a High-Resolution Digital Elevation Model in Gorce National Park, Poland. Scientific Reports 14: 14130. DOI: 10.1038/s41598-024-65026-z.

Szczęch M., Cieszkowski M., Chodyń R., Loch J., 2016. Geotouristic Values of the Gorce National Park and Its Surroundings (The Outer Carpathians, Poland). Geotourism/Geoturystyka 1-2(44–45): 27-40. DOI: 10.7494/geotour.2016.44-45.27.

Tsai W.N., Chen C.C., Chiang C.W., Chen P.Y., Kuo C. Y., Wang K.L., Lin M.L., Chen R. F., 2021. Electrical Resistivity Tomography (ERT) Monitoring for Landslides: Case Study in the Lantai Area, Yilan Taiping Mountain, Northeast Taiwan. Frontiers in Earth Science 9: 737271. DOI: 10.3389/feart.2021.737271.

Wężyk P., 2014. Guidebook for Courses of Use of LIDAR Products. National Office of Geodesy and Cartography: Warszawa.

Wrońska D., 2006. Wykształcenie i funkcjonowanie lejów źródliskowych potoków gorczańskich. Ochrona Beskidów Zachodnich 1: 59-65.

Wrońska-Wałach D., Płaczkowska E., Krzemień K., 2013. Leje źródłowe jako systemy morfodynamiczne w obszarach górskich. Przegląd Geograficzny 85: 31-51. DOI: 10.7163/przg.2013.1.3.

Wróbel M., Stan-Kłeczek I., Marciniak A., Majdański M., Kowalczyk S., Nawrot A., Cader J., 2022. Integrated Geophysical Imaging and Remote Sensing for Enhancing Geological Interpretation of Landslides with Uncertainty Estimation – A Case Study from Cisiec, Poland. Remote Sensing 15: 238. DOI: 10.3390/rs15010238.

Zakšek K., Oštir K., Kokalj Ž., 2011. Sky-View Factor as a Relief Visualization Technique. Remote Sensing 3: 398–415. DOI: 10.3390/rs3020398.